Unravelling corrosion degradation of aged aircraft components protected by chromate-based coatings

Cornet, A.J.; Homborg, A.M.; Ravi Anusuyadevi, P.; 't Hoen-Velterop, L.; Mol, J.M.C.

DOI
10.1016/j.engfailanal.2024.108070

Publication date
2024

Document Version
Final published version

Published in
Engineering Failure Analysis

Engineering Failure Analysis 159 (2024) 108070

Contents lists available at ScienceDirect

Engineering Failure Analysis

journal homepage: www.elsevier.com/locate/engfailanal

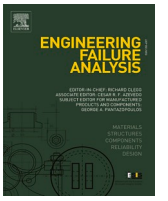

Unravelling corrosion degradation of aged aircraft components protected by chromate-based coatings

A.J. Cornet [a,b,*], A.M. Homborg [a,c], P.R. Anusuyadevi [a], L. 't Hoen-Velterop [d], J.M.C. Mol [a]

[a] Department of Materials Science and Engineering, Delft University of Technology, Mekelweg 2, 2628 CD Delft, Netherlands
[b] Royal Netherlands Air Force, Kooiweg 40, 4631SZ Hoogerheide, Netherlands
[c] Netherlands Defence Academy, Het Nieuwe Diep 8, 1781AC Den Helder, Netherlands
[d] National Aerospace Laboratory, Voorsterweg 31, 8316PR Marknesse, Netherlands

ARTICLE INFO

Keywords:
Aerospace engineering
Structures
Aluminium alloy
Composites
Fasteners
Microscopic characterization and microanalysis
Corrosion
Manufacturing defect
Isolation
Drain holes

ABSTRACT

Despite extensive research, eliminating hexavalent chromium-based inhibitors from aerospace coatings remains challenging due to a lack of understanding of coating degradation during aircraft service. This study addresses the issue by investigating the protective mechanisms and aging processes of chromate-containing coatings on aircraft components after service for over 35 years. Four aircraft parts underwent visual inspection, disassembly, and analysis using scanning electron microscopy (SEM) and X-ray Photoelectron Spectroscopy (XPS). While most coating areas remained intact after extended use, three distinct degradation modes were identified: tip erosion, corrosion around rivets, and corrosion around fasteners at the leading edge. These findings reveal the complexity of corrosion protection, emphasizing that hexavalent chromium-containing coatings may not offer comprehensive protection at local design heterogeneities. The study also highlights the need to revisit traditional laboratory analysis protocols based on accelerated corrosion testing of oversimplified sample configurations, given the revealed end-of-service failure mechanisms.

1. Introduction

Aluminium alloys persist as a primary construction material in the aerospace industry, chosen for their exceptional high strength-to-weight ratio, excellent ductility, very good manufacturability, high damage tolerance and fracture toughness, good elastic stiffness and modest price [1]. However, the complex microstructures inherent in these alloys render them highly susceptible to local corrosion, presenting significant challenges to the integrity in diverse applications, as critical-sized corrosion locations may also represent stress concentrations under static and dynamic mechanical loading conditions [2,3]. Recognizing this vulnerability underscores the critical need for effective corrosion mitigation strategies.

To address the corrosion issues, a prevailing approach involves the application of organic coatings [2]. These coatings serve as a robust physical barrier, protecting the aluminium alloy against the deleterious influences of the external environment. The success of this strategy is contingent upon an intact coating; however, real-world scenarios often involve situations where coatings will be

* Corresponding author at: Department of Materials Science and Engineering, Delft University of Technology, Mekelweg 2, 2628 CD Delft, Netherlands.
E-mail address: A.J.Cornet@TUDelft.nl (A.J. Cornet).

https://doi.org/10.1016/j.engfailanal.2024.108070
Received 11 January 2024; Received in revised form 25 January 2024; Accepted 1 February 2024
Available online 7 February 2024

damaged. In response to this vulnerability, contemporary coating technologies incorporate an active protection technology based on leaching corrosion inhibitors [2,3].

This active protection technology is crucial for preserving aluminium alloys against corrosion threats in the presence of coating defects. Over many decades, inhibitors, mainly rooted in chromates, have offered the active corrosion protection. Upon diffusion of a corrosive electrolyte into the organic coating, chromate leaches from the coating matrix into a damaged area, where it creates a protective, passive chromium-oxide layer at the exposed aluminium surface [4–8]. This mechanism prevents excessive corrosion damage to occur and preserves the overall structural integrity of the material.

Despite the effective use of chromate-containing coatings on aluminium aircraft parts, corrosion and fatigue remain the primary contributors to structural failure in aircraft [9–11]. Corrosion manifest in various forms observed during aircraft operation, including galvanic corrosion, exfoliation corrosion, pitting corrosion, crevice corrosion, etc. [11–13]. Failures in coating systems often play a major role in the occurrence of these various corrosion types in structural aircraft parts [14,15]. Coating failures are predominantly observed at overlapping joints, which involve differences in metal compositions and which can lead to the formation of crevices, creating an environment susceptible for corrosion. The combined influence of diverse environmental conditions and the increased susceptibility to erosion at these overlapping joints further amplifies their vulnerability to corrosion [9,12,15].

Whereas existing literature primarily focuses on corrosion in overlapping zones related to conventional aluminium-to-aluminium configurations combined with fasteners of different materials, it is crucial to recognize that contemporary designs incorporate an even more extensive array of materials. The integration of carbon fibre-reinforced polymer (CFRP) with aluminium alloys intensifies the overall susceptibility to corrosion [16]. Empirical evidence derived from corrosion tests [17,18] supports the susceptibility for corrosion in these cases, whereas a limited number of case studies demonstrate their vulnerability in aircraft during service [19]. This is one of the important reasons why the present case study was conducted: to gain a deeper understanding of corrosion propagation in such complex corrosion-sensitive designs. Aircraft parts were analysed after service, offering insights into the specific operational conditions that new coating formulations must withstand.

The intricacy introduced by these new designs presents challenges for corrosion engineers to propose effective corrosion protection schemes. This challenge is exacerbated by the fact that the use of chromates has raised significant concerns regarding potential health risks. These health risks are particularly relevant to individuals involved in aircraft painting and maintenance. Exposure to chromates by skin contact, inhalation or digestion may impose severe health issues when entering the cells of the human body as it has the capacity to harm the nucleus, which houses the DNA, possibly leading to genetic changes [20]. Additionally, chromates classification as a carcinogenic substance emphasizes its potential to elevate the risk of cancer among those who are exposed [21–23].

Given these health risks, the continued use of chromates in paint systems is no longer considered as a sustainable corrosion protection strategy for the future. Moreover, stringent international health and safety regulations have been implemented, exemplified by the prohibition of chromates since September 2017 under the Registration, Evaluation, Authorization, and Restriction of Chemicals (REACH) regulation [24]. This has sparked extensive research to seek viable alternatives to chromates [4,25–27]. Fortunately, several substitute inhibitors have been found and are already being incorporated into new coating systems. These alternative coating systems have been certified and are widely used to protect the exterior surfaces of aircraft [28]. However, for structural applications, i.e. the inside of the aircraft, the aerospace industry has been hesitant to fully embrace these alternative coatings. This reluctance stems from the unproven performance of these newly developed coatings under harsh service conditions at hard-to-reach aircraft interior locations where replacement of coatings is not feasible. Consequently, to date, chromates have remained to represent the exclusive chemical substance providing active corrosion protection by coatings for structural applications within the aerospace industry.

In the search for alternative coating systems, extensive efforts are being made to develop reliable methods for testing the performance of coating systems [28]. The aim is to accelerate the aging process in a representative manner and to assess how well newly developed coatings withstand corrosive conditions over time in comparison to their chromate containing counterparts. However, it has been difficult to establish a correlation between accelerated aging tests and real-world performance. Even the study of coatings during outdoor exposure has presented challenges in establishing a definitive correlation to in-service performance [29,30].

To enhance understanding and further develop hexavalent-chromium-free inhibitor alternatives, it is imperative to delve deeper into the process of coating degradation. Instead of solely relying on laboratory and accelerated testing methods, this research aims to study the actual deterioration of chromate containing paint systems under real-life service conditions. A more profound comprehension of degradation mechanisms can guide the selection of appropriate stressors in accelerated testing, ultimately enhancing the correlation with in-service exposure and performance [31]. While (quasi) in-situ investigation of coating degradation during service would be preferred, it poses formidable operational challenges, the authors anticipated to still gain valuable insights and information by conducting a post-mortem investigation after service.

By utilizing initial visual inspection and subsequent scanning electron microscopy (SEM) and energy dispersive x-ray (EDX) analysis, samples of real, used aircraft parts are studied. The aim of this forensic study is to unravel the (local) mechanisms of degradation and corrosion that had occurred over extended periods of service and serves to understand which degradation mechanisms contribute to the decrease in corrosion protection of chromate-containing coating systems during their actual service life.

2. Method

The research approach employed in this work encompasses several key steps, including the selection of aircraft parts, disassembly procedures, visual inspections and advanced microscopic and spectroscopic analysis techniques.

2.1. Selection of aircraft parts

Several aircraft part selection criteria were thoughtfully considered to ensure alignment with the research objectives. Firstly, the part opted for study was significantly aged and nearing the end of its service life. This allows the examination of the effects of prolonged exposure to environmental factors. Secondly, the degradation of the chosen part had to reflect the contemporary challenges faced in the aerospace industry, providing insight in current coating degradation issues. Thirdly, the availability of multiple identical parts, each with different flight hours and ages, allows to analyse the impact of use and aging profile on coating degradation. Ultimately, it was crucial that the coating scheme remained untouched throughout the part's entire lifespan, ensuring an accurate assessment of the original coating condition.

Four aircraft parts meeting the specified criteria were selected. These parts all had accumulated over 35 years of service, offering a diverse range of flight hours, thus representing real-world scenarios. An overview of this information is presented in Table 1.

2.2. Aircraft part description

Despite their age, the selected aircraft parts feature a modern design, comprising a CFRP skin and a structure fabricated from AA2024-T62, a legacy of high strength aerospace aluminium alloy. The skin and the structure are connected using stainless steel rivets, which are wet-installed with sealant to ensure the structural integrity of the components, as depicted in Fig. 1. This design, while lightweight and robust, presents a challenge due to the differences in electrochemical nobility of the materials used, making these parts potentially susceptible to galvanic corrosion, which is a contemporary challenge in the aerospace industry [32,33]. Additionally, the leading edge of the aircraft part is securely fastened using cadmium-plated steel screws, wet-installed with sealant.

Notably, the interior coating system, applied on the aluminium structure of these aircraft parts has remained unaltered throughout its extensive service life. The investigation, based on blueprints and SEM analysis, revealed that the corrosion protection system consists of two layers: The first layer consists of a chromic acid anodization layer with a thickness of approximately 2 μm (MIL-A-8625, Cl I), serving as a pretreatment. The second layer is composed of a strontium chromate primer (MIL-PRF-23377) with a thickness of approximately 25 μm.

2.3. Disassembly

The disassembly process is a critical step which involves the careful unscrewing of all screws to remove the leading edge. In cases where rusted screws were encountered, precise drilling was performed to ensure smooth and accurate disassembly. The subsequent step involves the delicate removal of the aircraft part's skin by extracting the stainless steel rivets. The extraction of these rivets involves precision drilling in their heads, followed by removal using a punch. Following the rivet removal, the skin is delicately separated from the aluminium structure, utilizing plastic scrapers to cut through the sealant. This meticulous disassembly procedure grants access to the internal coated aluminium structure, enabling the investigation of various forms of degradation within the aircraft part.

2.4. Visual inspection

Following the disassembly, a thorough visual inspection was conducted, to identify areas exhibiting signs of coating degradation. These specific areas were marked for further investigation using more advanced analytical techniques like SEM-EDX.

2.5. Material analytical techniques

SEM combined with EDX analysis was the primarily used analytical technique in this forensic research approach. The SEM analysis was performed utilizing the Thermo Scientific™ Helios™ UXe DualBeam G4, equipped with an EDX detector and a Focused Ion Beam (FIB). The FIB played a vital role in cross-sectional imaging of the coated samples within the SEM. Prior to using this method, challenges were encountered during wet polishing steps of embedded samples, where the release of strontium chromate led to the formation of pores which would affect the inspection results. By utilizing the FIB-milling process, this potential experimental artefact issue was successfully addressed.

For the SEM analysis, an acceleration voltage of 5 kV was utilized in both the secondary electron (SE) mode and the backscatter electron (BSE) mode to collect data and to be able to investigate the morphology of the coating. For EDX imaging, an acceleration voltage of 15 kV was employed to obtain elemental information. To minimize static charging effects within the SEM, non-conductive samples were coated with a thin layer of carbon, approximately 20 nm in thickness.

Table 1
Overview of the selected aircraft parts.

Part #	Flight Hours	Year of manufacturing
#2547	2547 FHR	1984
#4215	4215 FHR	1983
#5183	5183 FHR	1983
#5903	5903 FHR	1985

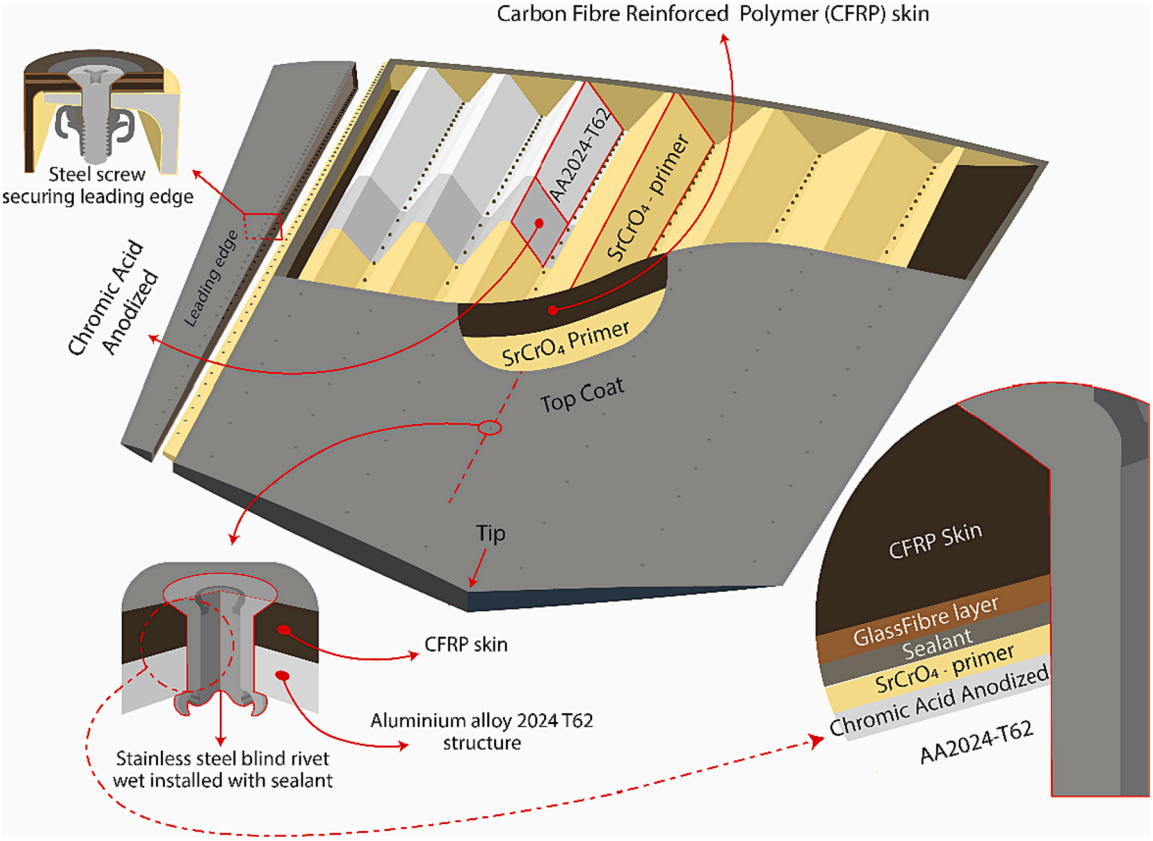

Fig. 1. Structural overview of inspected aircraft part.

For the analysis of deposited dust inside aircraft part, samples were collected using double sided copper tape and subjected to examination using SEM-EDX to determine the composition of the dust.

The surface chemistry of the aircraft part's tip was examined through X-ray Photoelectron Spectroscopy (XPS). The analyses were conducted utilizing a PHI-TFA XPS spectrometer from Physical Electronic Inc., featuring an Al Kα X-ray monochromatic source (hv = 1486.7 eV). Maintaining a vacuum of approximately 10^{-9} mbar during the XPS analysis, the pass energy for the survey was set at 89.45 eV.

Throughout the measurements, a circular area with a diameter of 0.4 mm was analysed and the depth of analysis was 3–5 nm. High-resolution multiplex scans of C *1 s*, O *1 s*, Al *2p*, and Cr *2p* peaks were collected, employing pass energy of 71.55 eV. These scans exhibited a resolution of 0.2 eV, with a 45° take-off angle. Exceptionally, the chromium spectrum was captured at an even higher resolution of 0.1 eV. All the obtained spectra underwent processing using MultiPak v.8.0, a software tool developed by Physical Electronics Inc., facilitating precise curve fitting. However, prior to curve fitting, all spectra were adjusted based on the C *1 s* spectra, setting the peak maximum of C *1 s* spectra to 284,8 eV [34].

3. Results and discussion

In this section, the results obtained from both the visual inspection and the subsequent SEM-EDX analysis of the aged aircraft parts are presented.

During the visual inspection of the four aged aircraft parts, it became apparent that the majority of the coating appeared to be in an excellent condition, showing no visible signs of degradation. Overall, only minor corrosion damage was detected. However, closer examination revealed three distinct degradation modes of particular interest:

(i) **Erosion at the tip:** erosion at the tip of the aluminium structure could be observed, accompanied by a deposition of grey dust.
(ii) **Corrosion around stainless steel rivet holes:** corrosion was present around several stainless steel rivet holes.
(iii) **Corrosion around stainless steel fasteners at the leading edge:** the fastener holes of the leading edge were surrounded by severe corrosion.

Further investigation of the intact areas and each of the specific corrosion cases unravelled the underlying causes behind these phenomena, presented in the following subsections.

3.1. The intact coating

To gain a deeper insight, SEM-EDX was employed to examine the coating, as shown in Fig. 2.

EDX was used to further analyse the elemental composition of different particles present in the coating. The EDX image shown in Fig. 2c reveals the presence of talc particles ($Mg_3Si_4O_{10}(OH)_2$), diatoms (as SiO_2), titanium oxide (TiO_2) and strontium chromate ($SrCrO_4$). Notably, the intact coating exhibited an almost pristine condition, with no observed pores, except in specific instances where pores were found around a scratch in the top layer of the primer. This observation implies a limited exposure to electrolytes, as particle leaching would typically occur under such conditions [35]. These small levels of electrolyte exposure could be attributed to the design of drain holes in the aircraft part, facilitating the easy exit of moisture and thereby potentially playing an important role in the corrosion protection. This analysis of the undisturbed coating area indicates that the hexavalent chromium coatings provided excellent corrosion protection in the featureless plain field areas of the aircraft components under investigation.

3.2. Erosion at the tip

In this section, the eroded areas at the tip of the aluminium structural aircraft parts are investigated. Through visual examination, cross sections were scrutinized using SEM, ranging from the intact parts of the coating to severely damaged regions. This is depicted in Fig. 3. Interestingly, these findings indicate that despite the damage extending down to the bare metal in “area E”, no apparent signs of corrosion are evident.

In order to elucidate the reasons behind this lack of corrosion, EDX images were acquired and analysed, specifically in areas (B) and (C) as shown in Fig. 3. The resulting EDX images are presented in Fig. 4. Analysis of these images revealed a notable presence of chromium remaining within the coating. However, some chromium is leached out as observed in Fig. 4c and 4f. This finding, including the findings of the intact coating, implies relatively dry conditions during service, despite periodic humid cycling and extended rainy periods during its service life under conditions where humidity levels exceed 90 % for over a week. These conditions might have induced minor moisture ingress into the coating, which triggered the leaching of chromate around the damaged area at the tip.

Considering these observations, it is plausible to hypothesize that the leaching of chromate may have played a protective role for

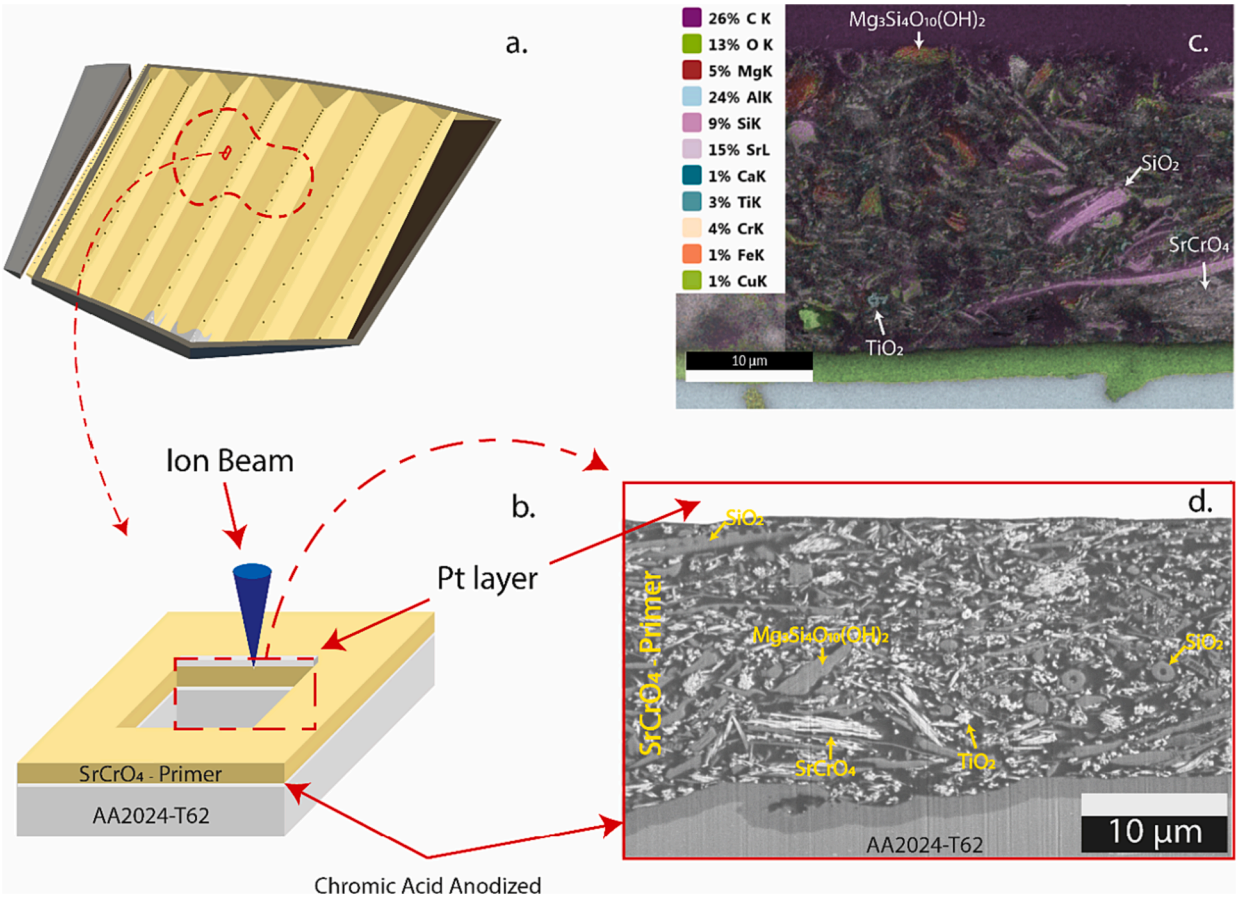

Fig. 2. Cross-sectional view of an intact coating achieved through FIB milling: (a) sample location within the overall aircraft part studied; (b) FIB-milling preparation method; (c) cross-sectional EDX mapping image; (d) cross-sectional BSE microscopic image.

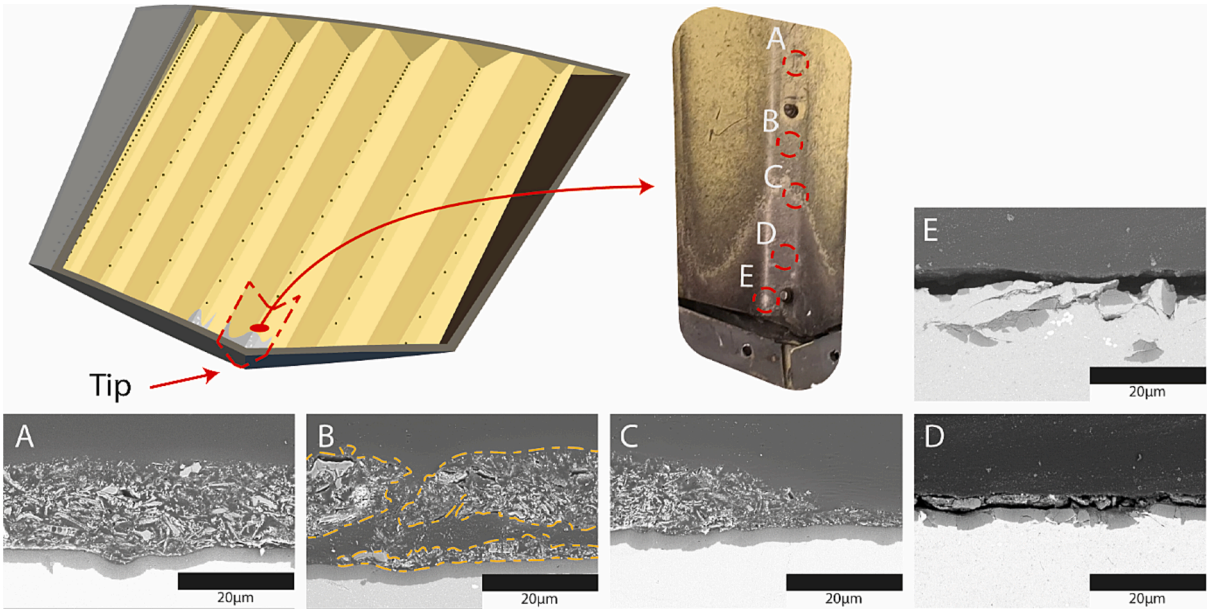

Fig. 3. SEM cross-sectional images illustrating distinct degradation stages observed in eroded areas at the tip: (a) intact coating; (b) adhesive and cohesive failure; (c) coating partly eroded; (d) only anodized layer intact; (e) local erosion down to bare metal.

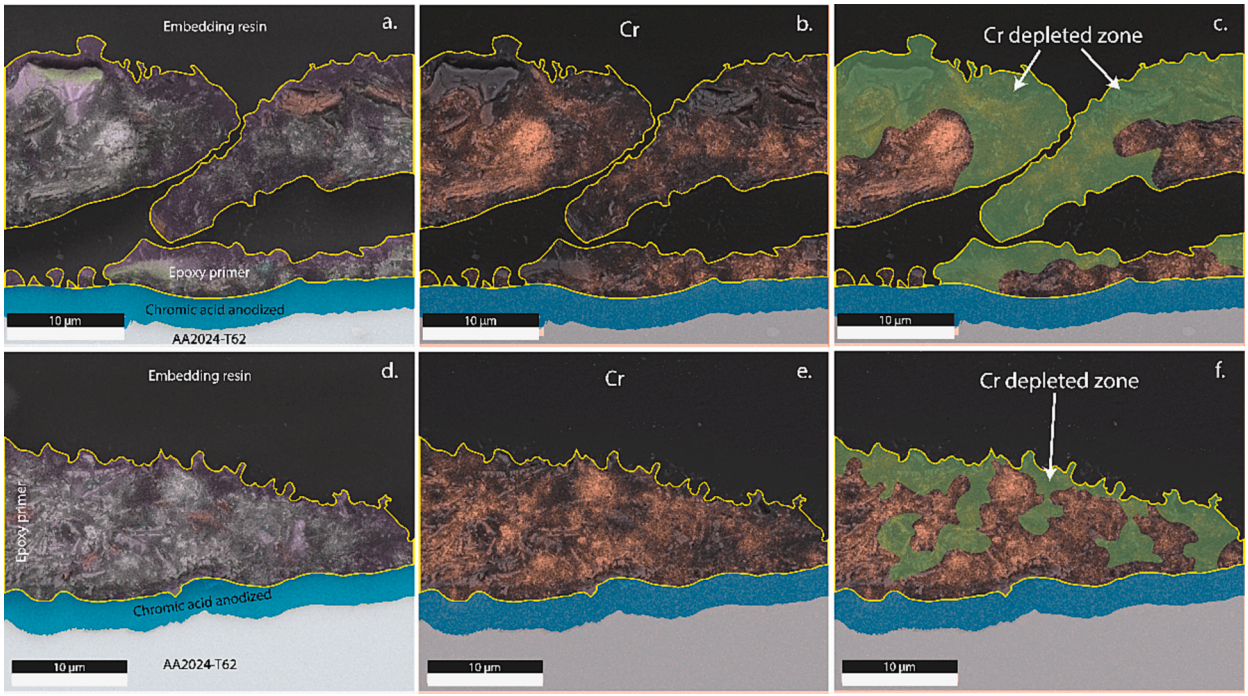

Fig. 4. SEM-EDX images revealing the coating conditions in eroded areas: (a) exhibiting adhesive and cohesive failure, accompanied by its corresponding image (b) illustrating chromium distribution; (c) revealing the chromium-depleted zone; (d) showcasing the coating erosion interface, along with its corresponding image (e) highlighting chromium distribution and in (f) the chromium-depleted zone.

the exposed bare aluminium surfaces during service, particularly in a moderately corrosive environment. To explore this hypothesis further, additional investigation using XPS was conducted.

The high-resolution spectra, depicted in Fig. 5, reveals distinctive peaks corresponding to the elements of aluminium (Al 2*p*), oxygen (O 1 *s*) and chromium (Cr $2p_{3/2}$). Fitting and analysis of the obtained spectra provides valuable insights. The aluminium spectrum (Fig. 5b) indicates the primary presence of aluminium- and copper-oxide, confirming the presence of the aluminium alloy

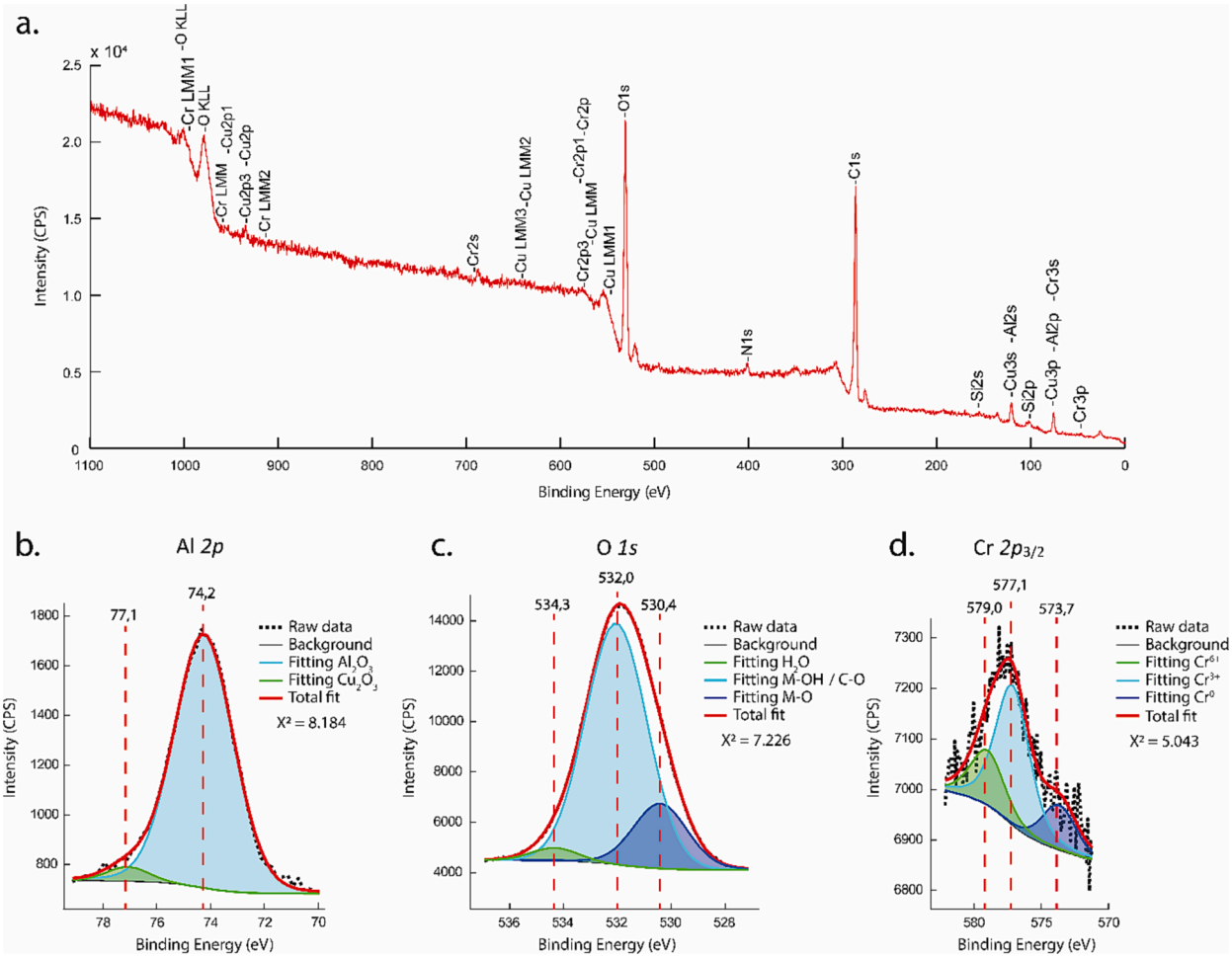

Fig. 5. XPS survey spectrum (a), including fitted outcomes in the high resolution spectra, obtained from the region at the tip of the investigated aircraft component, elucidating the elements (b) aluminium, (c) oxygen, and (d) chromium.

AA2024-T62 in the bare aluminium regions [36–38]. The broad Al 2*p* spectrum also encompass contributions from aluminium hydroxides ($Al(OH)_3$ and AlO(OH)) [37]. To gain a deeper understanding of the varying amounts of metal oxides and hydroxides, the oxygen spectrum is further analysed.

The fitted oxygen spectrum (Fig. 5c) reveals the presence of H_2O, metal hydroxides (e.g., aluminium and chromium hydroxides), and metal oxides [37,39–41]. The heightened concentration of aluminium oxide is attributed to the damaged anodized oxide layer as observed in the bare aluminium surfaces (Fig. 3e). The presence of metal hydroxide bonds can be ascribed to the corrosion of the aluminium alloy and the sealing treatment after anodizing, both resulting in aluminium hydroxide. The metal hydroxide bonds can further be attributed to chromium hydroxide, as indicated by the distinctive chromium peak in the Cr $2p_{3/2}$ spectrum, as depicted in Fig. 5d.

Notably, the assigned chromium peak specifically identifies hexavalent chromium, trivalent chromium and chromium metal. Hexavalent chromium can be attributed to leached strontium chromate, while trivalent chromium can be linked to chromium hydroxide, indicating the presence of a protective layer in the bare aluminium regions [41–46]. This lends support to the hypothesis that the leaching of strontium chromate particles from the coating resulted in the formation of a protective layer of chromium hydroxide onto which hexavalent chromium is adsorbed, forming Cr^{3+}-O-Cr^{6+} bonds over the intermetallic particles of the aluminium alloy AA2024-T62. This nanolayer, along with the aluminium hydroxide with adsorbed hexavalent chromium (Al^{3+}-O-Cr^{6+}), formed over the remaining aluminium in the alloy offers protection against corrosion [7,8,47]. However, the origin of the fitted Cr^0 spectra, indicating the presence of chromium metal, remains unclear and cannot be attributed to traces of stainless steel, as no traces of iron and nickel are found in the survey spectrum.

Continuing the investigation, the grey deposited dust atop the eroded areas was also investigated. The EDX analysis of the grey deposited dust clearly unveiled its predominant composition, arising from identifiable coating particles marked by the presence of C, Si, and Sr. Furthermore, traces of sealant, characterized by S and Ca, were identified, along with traces of stainless steel, distinguished by the presence of Fe, Ni, and Cr. These elements were discerned within the deposited dust, alongside aluminium oxide originating

from the anodized oxide layer as depicted in Fig. 6.

Furthermore, a notable observation was made of physical pieces of rivets within the aircraft parts. This finding lends further support to the presence of stainless steel particles and strongly suggests that the damage observed in the eroded areas is the result of the rivets eroding the surface at the tip of the aluminium structure over the course of its service life.

These rivet particles found inside the part may have entered during the manufacturing process. When incorrectly installed rivets require replacement, the head of the rivet is removed and the remaining part is pushed through the outer skin using a punch. In this way, the remains of the rivet may drop inside the part and adhere to the structure, due to the presence of wet sealant. This is shown in Fig. 7. Over time, during operational service these particles may detach, become mobile and potentially cause erosion of the coating at the tip.

In summary, the investigation into erosion at the tip highlighted multiple contributing factors to the degradation mechanism, including the moisture uptake, the protective role of chromate and the potential impact of rivet particles left over from the manufacturing process.

3.3. Corrosion around stainless steel fasteners

The forensic investigation revealed corrosion attack around stainless steel blind rivets used to attach the skin to the aluminium structure. It was found that the aluminium structure at the perimeter of these rivets exhibited exfoliation corrosion, which is shown in Fig. 8. It appears that this corrosion damage is partially induced by crevices surrounding the rivets, as well as by galvanic potential differences among the various materials involved. Cracks in the coating around the corroded rivets further support this hypothesis. This visual evidence is presented in Fig. 9, where the corroded rivets are clearly visible with a black oxide film on top of the coating, which is commonly referred to as “smoking rivets” in the aviation industry [48,49].

It can be hypothesized that moisture enters the component through the cracks surrounding the rivets, acting as an electrolyte. This moisture penetrates along the rivet interface, deeper between the CFRP skin and the aluminium structure. As a result, this creates conditions for galvanic as well as crevice corrosion to occur. Additionally, when moisture comes into contact with the coating and diffuses into it, this causes the leaching of chromate, which slows down the corrosion process. The next section will describe the specific mechanisms involved, as there are similarities between the corrosion mechanisms observed around steel fasteners at the leading edge.

3.4. Corrosion around steel fastener at the leading edge

In one particular case, on part #5903, severe corrosion was observed around steel screws holding the leading edge in place. The corrosion was predominantly found on the aluminium spar and primarily exhibited exfoliation, as shown in Fig. 10. Additionally, a crack was identified in the coating surrounding the corroded fasteners, providing an entry point for moisture to penetrate into the component. Even the steel anchor nuts exhibited significant corrosion. This is an uncommon occurrence considering the connection of steel fasteners with the aluminium structure. The steel typically benefits from the protective nature of aluminium in the case of electrical contact. This aspect will be further discussed in this section.

The corrosion around steel fasteners at the leading edge showed similarities to the corrosion observed around the stainless steel blind rivets. What sets this case apart is the absence of a dedicated drain hole in the area, allowing moisture to accumulate and exacerbate the corrosion process.

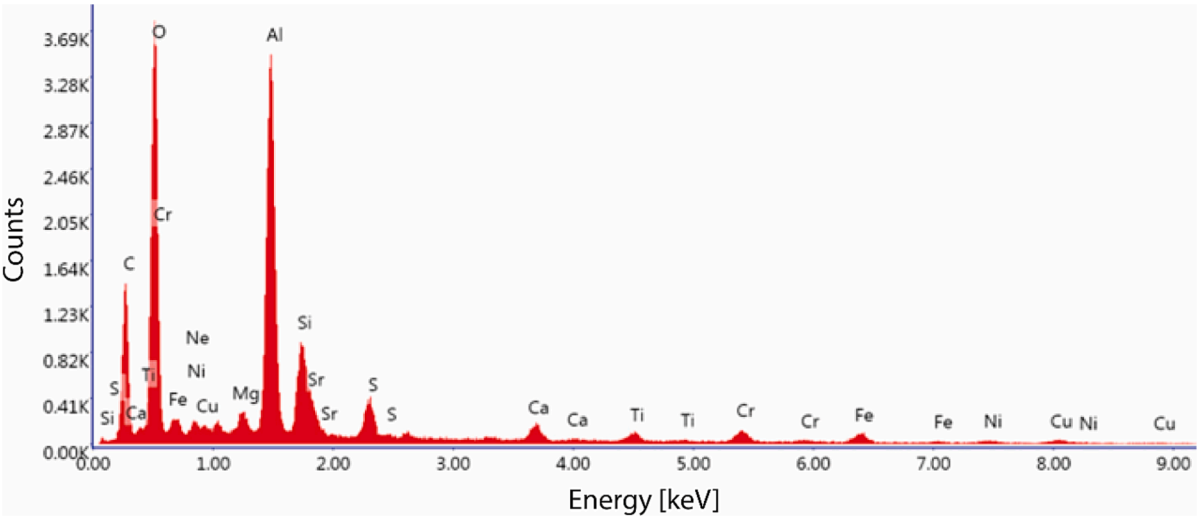

Fig. 6. EDX analysis of grey deposited dust discovered in the eroded areas of the aircraft component.

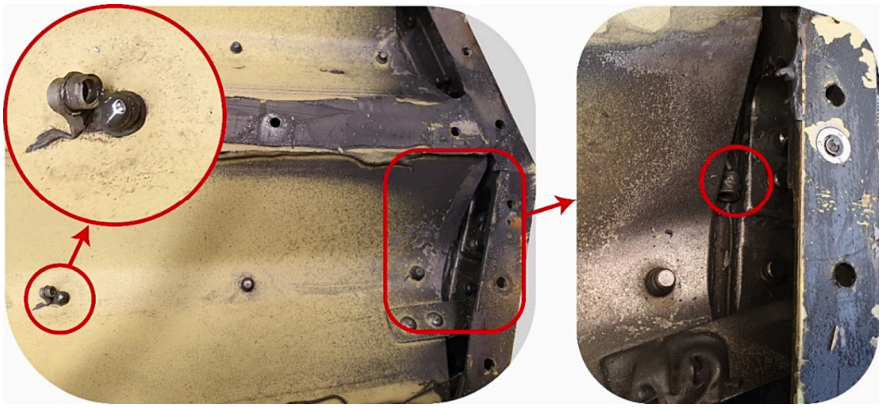

Fig. 7. Pieces of stainless steel blind rivets, found at the tip of the aircraft part investigated.

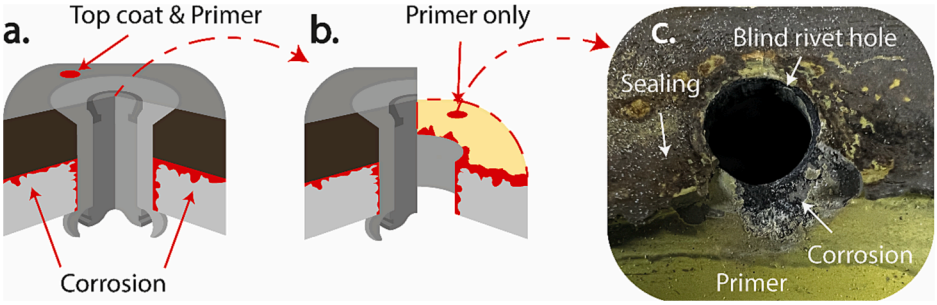

Fig. 8. Corrosion evident near the stainless steel blind rivet, utilized for connecting the CFRP skin to the aluminium structure, featuring (a) a cross-sectional view of a blind rivet; (b) the specified field of view for image (c); (c) highlighting the corrosion attack in and around the rivet hole.

This issue was observed only once. Therefore, it is important to investigate differences with other parts to determine why this occurred in this case. It was observed that in contrast to part #5903, other aircraft parts exhibit a stroke of sealant covering the screw heads. This sealant stroke, measuring approximately 1 mm in thickness and 25 mm in width, serves as an effective barrier against moisture penetration through the fastener interface. Surprisingly, this stroke of sealant was not applied to part #5903, which strongly suggests that moisture ingress through the fastener interface was the root cause.

To gain a deeper understanding of the mechanisms involved, a detailed examination using SEM-EDX was conducted. This analysis focused on a cross-section of a corroded fastener, paying special attention to the area where both the paint and the aluminium spar had degraded, as depicted in Fig. 11. The SEM-EDX images in Fig. 11 reveal different layers, or regions. In Fig. 11e and 11f the corroded aluminium spar is visible, covered by the chromic acid anodized layer. On top of the chromic acid anodized layer the remains of the coating are present. Additionally, aluminium corrosion products were observed on top of the structural primer of the aluminium spar, surrounded by the sealing which was additionally applied between the coated aluminium spar and the CFRP skin.

Fig. 11f shows the presence of a Cr depletion front inside the coating: at the left-hand side, chromate is present in the coating, whereas at the right-hand side the chromate is almost entirely depleted. Additionally, this Cr depletion front appears to be present in the aluminium spar, with a clear distinction between the pristine material at the left-hand side and the corroded area at the right-hand side. This is a strong indication that moisture ingress had taken place while chromate slowly dissolved when it came into contact with moisture. The same also applies to the corrosion itself, with the presence of electrolyte as an essential condition.

Additional EDX images reveal the distribution of chromium and aluminium, as seen in Fig. 12. Notably, chromium is mainly present in the corroded aluminium of the spar, indicating its functionality to protect the aluminium and to prevent further corrosion. Additionally, aluminium is observed inside the coating itself. This is remarkable since in principle this type of coating does not contain any aluminium particles.

Based on these findings, the sequence of events and mechanisms involved can be reconstructed. Initially, a depletion front inside the coating indicates the presence of moisture. The moisture trapped in the crevice electrolytically connects dissimilar metals, initiating the corrosion process. This results in the oxidation of the aluminium spar. It can be inferred that the concurrent reduction reaction takes place at or near the head of the bolt, given the apparent presence of an electrolyte at the bolt head and the flow of electrons from the aluminium spar towards the bolt [50,51]. The electrical connection between the bolt and the spar likely results from the tightening process, as metal-to-metal contact is hard to avoid, even when wet installed with sealant.

When moisture comes into contact with a coating, it slowly penetrates into the coating along the pores and the polymer matrix [52–54]. If the moisture comes into contact with strontium chromate, it dissolves and strontium ions as well as chromate ions, either as

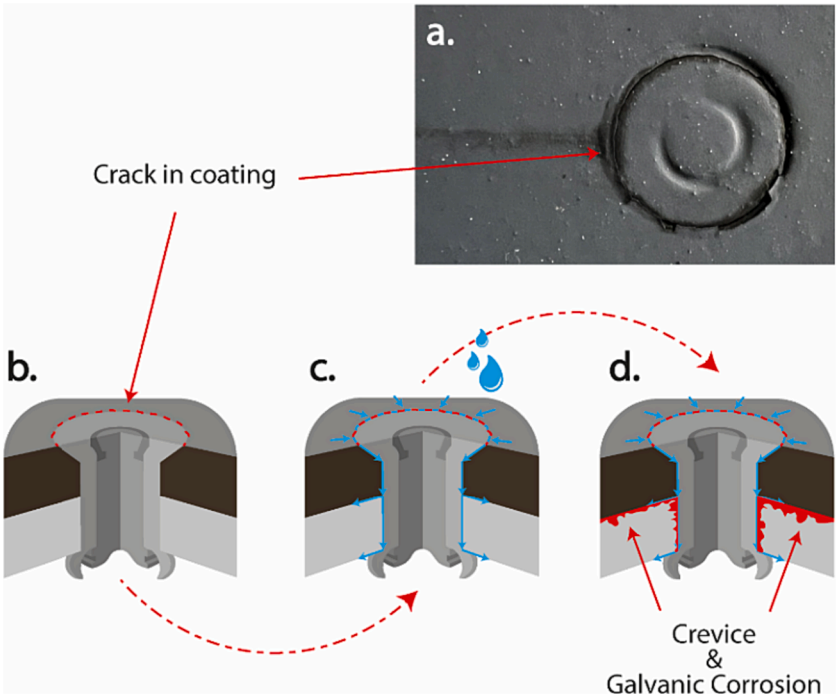

Fig. 9. Visualization of cracks encircling stainless steel blind rivets and a corrosion tail (a) depicting the hypothesized sequence; (b) initiation of a crack in the coating surrounding the rivet; (c) infiltration of moisture through the crack, penetrating around the rivet into the part; (d) resulting in corrosion of the aluminium structure.

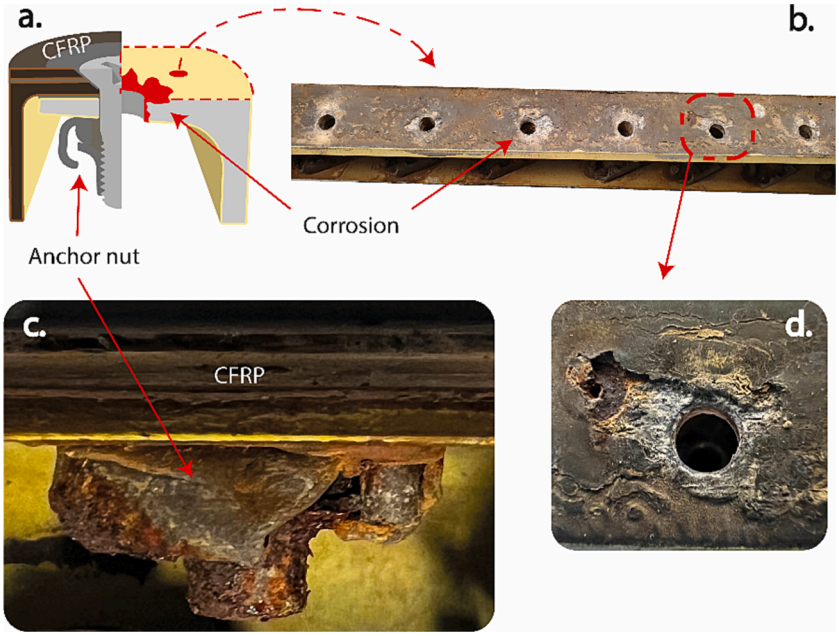

Fig. 10. Corrosion observed at the aluminium leading edge spar of #5903, with (a) illustrating the design detail; (b) highlighting corrosion of the aluminium spar; (c) depicting corrosion on the anchor nut; and (d) offering a close-up view of corrosion around a fastener hole.

CrO_4^{2-} and/or as $Cr_2O_7^{2-}$ depending on pH, will leach out of the coating [55–59]. The soluble chromate, promoted by the oxidation of aluminium, undergoes a reduction to trivalent chromium according to the following reduction reaction: $CrO_4^{2-} + 4H_2O + 3e^- \rightarrow Cr^{3+} + 8OH^-$ [47]. The trivalent chromium in the solution undergoes hydrolysis, preferably over oxygen reduction sites, forming a monolayer of Cr^{3+} species [7,47,58,59]. This chromium (hydr-)oxide films cover the oxygen reduction sites

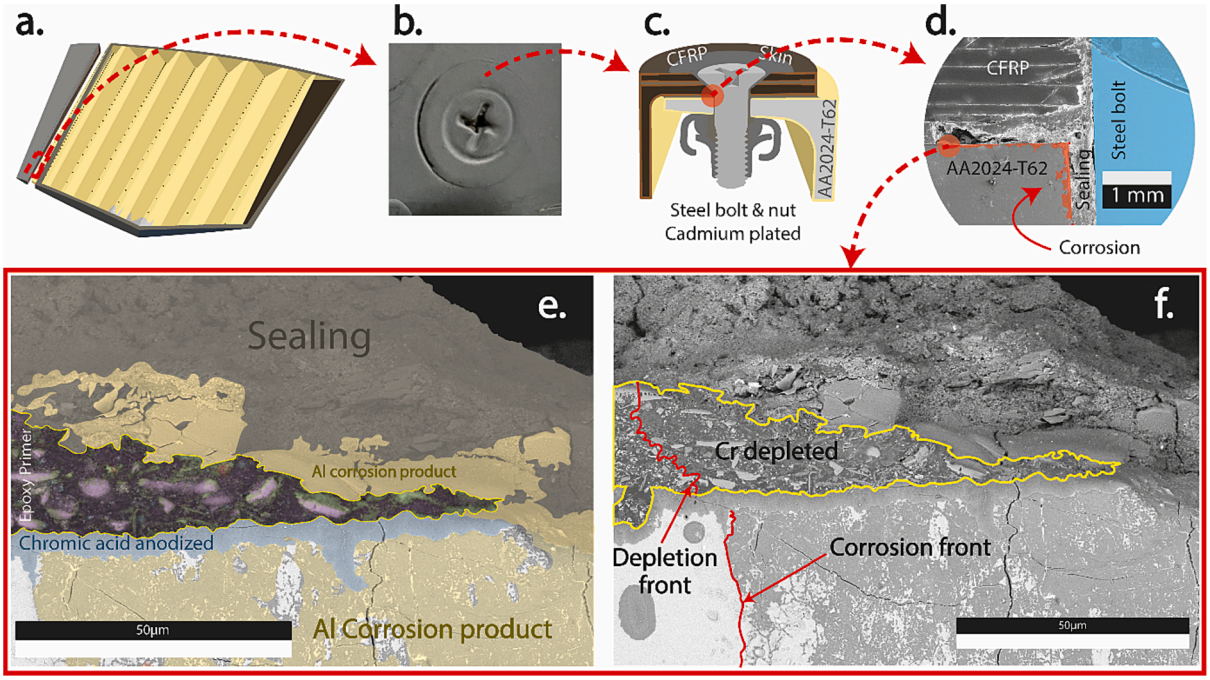

Fig. 11. SEM image of a cross-section of corrosion on the aluminium spar, where (a) presents the area of interest; (b) top view with a fastener installed; (c) graphical cross-section of an installed fastener; (d) low-magnification SEM image of a cross-section of an installed fastener; (e) high-resolution SEM image including a graphical clarification of the substances observed; (f) SEM image including a clarification of the Cr-depletion zone and corrosion front.

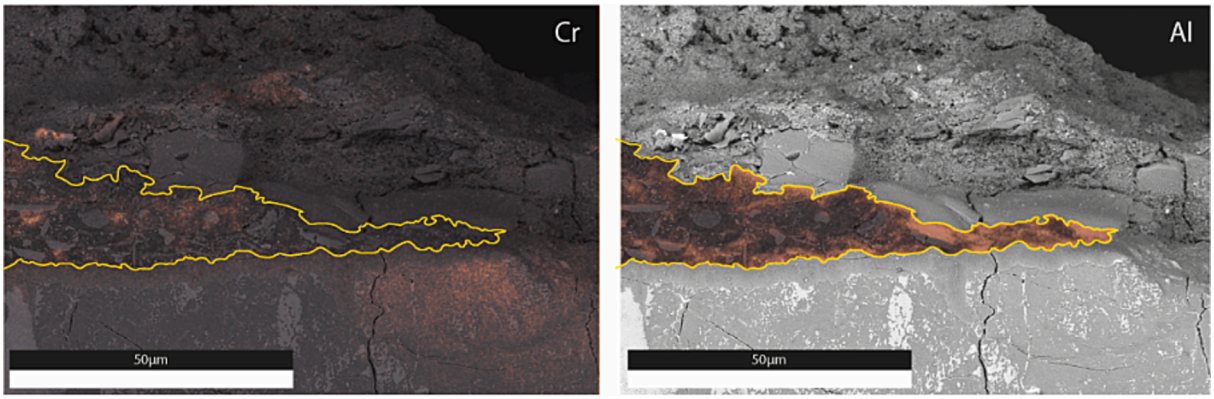

Fig. 12. EDX images showing Cr and Al distribution of the corroded aluminium spar.

and decelerate the reduction reactions [7,47,58–60].

Furthermore, at the active corrosion sites, hexavalent chromium is adsorbed. The chromates are specifically adsorbed at cathodic sites present over the chromium (hydr)oxide layer, generating Cr^{3+}-O-Cr^{6+} bonds [7,8,59]. Simultaneously, hexavalent chromium adsorbs at anodic sites on the aluminium (hydr-)oxide layer, resulting in the formation of Al^{3+}-O-Cr^{6+} bonds [7,59]. The adsorbed chromates actively contribute to the effectiveness of the passivation layer, forming a dipolar structure that impedes electron transfer, thereby enhancing the barrier properties [7,59]. Moreover, this results in a reduction of the zeta potential of the aluminium oxide, leading to decreased adsorption of chloride ions at the anodic sites [7]. In addition, this passivation layer hinders the adsorption of oxygen at the cathodic sites, which contributes to the outstanding passivation of aluminium alloys [7,8,58,59,61].

Based on the analysis of Fig. 12, it is confirmed that a substantial amount of chromium is found in the aluminium corrosion product inside the spar. The presence of rust on the anchor nut, as seen in Fig. 9, further supports the hypothesis of passivation of the aluminium spar, since the iron oxidation rate is limited if a less noble material like aluminium in an active state is in direct electrical contact with the bolt. However, the inhibition power of hexavalent chromium was insufficient to fully suppress corrosion of the spar.

Summarized, this study provides valuable insights into the connection between degradation modes and corrosion mechanisms. By

examining the observed exfoliation corrosion and the impact of crevice and galvanic corrosion mechanisms, the authors identify the role of degradation modes and stressors in driving the corrosion progression. The authors observed that the absence of drain holes and inadequately positioned sealing strokes around fasteners can lead to the accumulation of moisture and by this way exacerbate corrosion. These findings shed light on the sequence of events and the mechanisms involved in the observed corrosion issues.

4. Conclusion

The findings reported in this forensic study on the deterioration of coated interior aircraft parts throughout their service life strongly indicate the occurrence of crevice and galvanic corrosion mechanisms leading to exfoliation corrosion. The presence of exfoliation corrosion in the aircraft parts examined suggests that hexavalent chromium coatings are insufficient in preventing corrosion when driven by crevice and galvanic corrosion mechanisms. These aggressive mechanisms require alternative approaches for effective corrosion prevention. One such approach is the application of sealant over fastener heads, as was successfully performed for the leading edge. Additionally, the presence or absence of drain holes to prevent water accumulation in specific areas plays a role in corrosion prevention. Both measures effectively prevent water accumulation in enclosed compartments, thereby mitigating a critical failure mode. Moreover, this study also demonstrates the effectiveness of insulating materials between the CFRP skin and aluminium structure, emphasizing the importance of good design practices. The incorporation of insulating materials, whether through sealants or by the application of a glass fibre layer, eliminates electrical contact between different materials, thus mitigating galvanic corrosion. This underscores that a comprehensive corrosion prevention strategy should incorporate multiple individual measures, including a well-designed structure to prevent water ingress and water accumulation, and the application of galvanic isolation between different materials to improve their operational lifetime.

However, it should be noted that besides the specific examples discussed above, hexavalent chromium coatings exhibit excellent protection throughout the lifetime of the featureless plain areas of the analyzed aircraft components. This is evidenced by the intact state of the coatings and further supported by the analysis of the eroded areas at the tip of the aircraft parts. Even when the coating is eroded, the bare aluminium is still protected by the chromate leaching from the coating system.

The corrosion mechanisms investigated in this work are not typically observed in standardized accelerated corrosion tests which largely ignore local design details. The influence of the mismatch between accelerated tests and in-service performance as presented here remains unclear and was not part of the present work. However, detailed understanding of local corrosion mechanisms and their kinetics both in accelerated testing and under in-service conditions is crucial as these can largely determine the potential correlation between accelerated testing and real-life performance. Further investigation towards novel and adapted representative and relevant testing protocols for active protective aerospace coatings is therefore considered to be of pivotal importance.

CRediT authorship contribution statement

A.J. Cornet: Writing – original draft, Methodology, Investigation, Formal analysis. **A.M. Homborg:** Supervision, Writing – review & editing. **P.R. Anusuyadevi:** Data curation, Writing – review & editing. **L. 't Hoen-Velterop:** Supervision, Writing – review & editing. **J.M.C. Mol:** Supervision, Writing – review & editing.

Declaration of competing interest

The authors declare that they have no known competing financial interests or personal relationships that could have appeared to influence the work reported in this paper.

Data availability

Data will be made available on request.

Acknowledgment

The Logistic Centre Woensdrecht of the Royal Netherlands AirForce is gratefully acknowledged for enabling this research and accommodating the research work, respectively.

References

[1] V.V.K. Prasad Rambabu, N. Eswara Prasad, R.J.H. Wanhill, Aerospace Materials and Material Technologies, Volume 1: Aerospace Material Technologies, Aerospace Materials and Material Technologies Volume 1: Aerospace Materials 1 (2017) 586. 10.1007/978-981-10-2134-3.
[2] A.E. Hughes, N. Birbilis, J.M.C. Mol, S.J. Garcia, Z. Xiaorong, G.E. Thompson, High Strength Al-Alloys: Microstructure, Corrosion and Principles of Protection, Recent Trends in Processing and Degradation of Aluminium Alloys (2011). 10.5772/18766.
[3] T. Mills, S. Prost-Domasky, K. Honeycutt, C. Brooks, Corrosion and the threat to aircraft structural integrity, Corros. Control Aerospace Ind. (2009) 35–66, https://doi.org/10.1533/9781845695538.1.35.
[4] O. Gharbi, S. Thomas, C. Smith, N. Birbilis, Chromate replacement: what does the future hold? npj Mater. Degrad. 2 (2018) 23–25, https://doi.org/10.1038/s41529-018-0034-5.
[5] J. Sinko, Challenges of chromate inhibitor pigments replacement in organic coatings, Prog. Org. Coat. 42 (2001) 267–282, https://doi.org/10.1016/S0300-9440(01)00202-8.

[6] S. Zehra, M. Mobin, J. Aslam, Chromates as corrosion inhibitors, INC, 2021. 10.1016/B978-0-323-90410-0.00014-3.
[7] G.S. Frankel, C.R. Clayton, R.D. Granata, M. Kendig, H.S. Isaacs, R.L. McCreery, M. Stratmann, Mechanism of Al Alloy Corrosion and the Role of Chromate Inhibitors, (2001) 1–83.
[8] G.S. Frankel, R.L. McCreery, Inhibition of Al Alloy Corrosion by Chromates, Electrochem. Soc. Interface 10 (2001) 34–38, https://doi.org/10.1149/2.f06014if.
[9] H. Ali Khan, A. Shahid, S. Khushbash, A. Hameed, S. Zameer Abbas, Investigation of failure and development of mitigation techniques of a cracked aircraft wing spar cap, Eng. Fail. Anal. 147 (2023), https://doi.org/10.1016/j.engfailanal.2023.107149.
[10] A. Venugopal, R. Mohammad, M.F.S. Koslan, S.R.S. Bakar, A. Ali, The effect of tropical environment on fatigue failure in royal malaysian airforce (RMAF) aircraft structure and operational readiness, Materials 14 (2021), https://doi.org/10.3390/ma14092414.
[11] T. Mills, S. Prost-Domasky, K. Honeycutt, C. Brooks, Corrosion and the threat to aircraft structural integrity, (n.d.). 10.1533/9781845695538.1.35.
[12] M. Czaban, Aircraft corrosion - Review of corrosion processes and its effects in selected cases, Fatigue Aircraft Struct. 2018 (2018), https://doi.org/10.2478/fas-2018-0001.
[13] G. Singh, D. Singh, G.S. Dhindsa, G. Singh, P. Singh, Corrosion in Aircraft Components : Types, Impacts and Protection Measures, Int. J. Adv. Sci. Technol 29 (2020).
[14] T. Zhang, T. Zhang, Y. He, Y. Wang, Y. Bi, Corrosion and aging of organic aviation coatings: A review, Chin. J. Aeronaut. 36 (2023), https://doi.org/10.1016/j.cja.2022.12.003.
[15] L. Niu, X. Guo, Q. Si, S. Fu, X. Li, Risk Analysis of Organic Coating Failure on Aluminum-based Aircraft Skin, J. Eng. Sci. Technol. Rev. 15 (2022), https://doi.org/10.25103/jestr.153.05.
[16] F. Ahmad, M. Al Awadh, S. Noor, Optimum alternate material selection methodology for an aircraft skin, Chinese J. Aeronaut. 36 (2023). 10.1016/j.cja.2023.05.019.
[17] M.A. Karim, J.H. Bae, D.H. Kam, C. Kim, W.H. Choi, Y. Do Park, Assessment of rivet coating corrosion effect on strength degradation of CFRP/aluminum self-piercing riveted joints, Surf. Coat. Technol. 393 (2020) 125726, https://doi.org/10.1016/j.surfcoat.2020.125726.
[18] Y. Chen, M. Li, T. Su, X. Yang, Mechanical degradation and corrosion characterization of riveted joints for CFRP/Al stacks in simulated marine environments, Eng. Fail. Anal. 137 (2022), https://doi.org/10.1016/j.engfailanal.2022.106382.
[19] J.J.H.M. van Es, L. 't Hoen-Velterop, 2019 Department of Defense – Allied Nations Technical Corrosion Conference, (2019) 1–13.
[20] N.A. Azeez, S.S. Dash, S.N. Gummadi, V.S. Deepa, Nano-remediation of toxic heavy metal contamination: Hexavalent chromium [Cr(VI)], Chemosphere 266 (2021) 129204, https://doi.org/10.1016/j.chemosphere.2020.129204.
[21] D. Samantaray, S. Mohapatra, B.B. Mishra, Microbial Bioremediation of Industrial Effluents, Elsevier Inc., 2014. 10.1016/B978-0-12-800021-2.00014-5.
[22] C. Krawic, M.W. Luczak, A. Zhitkovich, Variation in extracellular detoxification is a link to different carcinogenicity among chromates in rodent and human lungs, Chem. Res. Toxicol. 30 (2017) 1720–1729, https://doi.org/10.1021/acs.chemrestox.7b00172.
[23] A.L. Holmes, S.S. Wise, J.P. Wise, Carcinogenicity of hexavalent chromium, Indian J. Med. Res. 128 (2008) 353–372.
[24] T. Santonen, H. Louro, B. Bocca, R. Bousoumah, R.C. Duca, A. Fucic, K.S. Galea, L. Godderis, T. Göen, I. Iavicoli, B. Janasik, K. Jones, E. Leese, V. Leso, S. Ndaw, K. Poels, S.P. Porras, F. Ruggieri, M.J. Silva, A. Van Nieuwenhuyse, J. Verdonck, W. Wasowicz, A. Tavares, O. Sepai, P.T.J. Scheepers, S. Viegas, The HBM4EU chromates study – Outcomes and impacts on EU policies and occupational health practices, Int. J. Hyg. Environ. Health 248 (2023), https://doi.org/10.1016/j.ijheh.2022.114099.
[25] R.L. Twite, G.P. Bierwagen, Review of alternatives to chromate for corrosion protection of aluminum aerospace alloys, Prog. Org. Coat. 33 (1998) 91–100, https://doi.org/10.1016/S0300-9440(98)00015-0.
[26] F. Peltier, D. Thierry, Review of Cr-Free Coatings for the Corrosion Protection of Aluminum Aerospace Alloys, Coatings 12 (2022) 1–27, https://doi.org/10.3390/coatings12040518.
[27] S. Zhao, N. Birbilis, Searching for chromate replacements using natural language processing and machine learning algorithms, npj Mater. Degrad. 7 (2023), https://doi.org/10.1038/s41529-022-00319-0.
[28] A.E. Hughes, J.M.C. Mol, M.L. Zheludkevich, R.G. Buchheit, Active Protective Coatings, 2016. 10.1007/978-94-017-7540-3_4.
[29] O. Knudsen, A.W.B. Skilbred, A. Løken, B. Daneshian, D. Höche, Correlations between standard accelerated tests for protective organic coatings and field performance, Mater. Today Commun. 31 (2022), https://doi.org/10.1016/j.mtcomm.2022.103729.
[30] J. Dante, Accelerated Dynamic Corrosion Test method Development, 2017.
[31] N. Lebozec, D. Thierry, Influence of climatic factors in cyclic accelerated corrosion test towards the development of a reliable and repeatable accelerated corrosion test for the automotive industry, Mater. Corros. 61 (2010) 845–851, https://doi.org/10.1002/maco.200905497.
[32] D. Snihirova, D. Höche, S. Lamaka, Z. Mir, T. Hack, M.L. Zheludkevich, Galvanic corrosion of Ti6Al4V -AA2024 joints in aircraft environment: Modelling and experimental validation, Corros. Sci. 157 (2019), https://doi.org/10.1016/j.corsci.2019.04.036.
[33] L.Z. Mikhail, K. Silvar, S. Maria, Protection of multimaterial assemblies, Phys. Sci. Rev. 1 (2019), https://doi.org/10.1515/psr-2015-0012.
[34] G. Greczynski, L. Hultman, Impact of sample storage type on adventitious carbon and native oxide growth : X-ray photoelectron spectroscopy study, Vacuum 205 (2022) 111463, https://doi.org/10.1016/j.vacuum.2022.111463.
[35] T. Bos, Prediction of coating durability - Early detection using electrochemical methods, 2008.
[36] W. Song, M. Yoshitake, S. Bera, Y. Yamauchi, Oxygen adsorption and oxide formation on Cu-9% Al(111) surface studied using low energy electron diffraction and X-ray photoelectron spectroscopy, Japanese J. Appl. Phys., Part 1: Regular Papers Short Notes Rev. Papers 42 (2003) 4716–4720, https://doi.org/10.1143/jjap.42.4716.
[37] J.T. Kloprogge, L.V. Duong, B.J. Wood, R.L. Frost, XPS study of the major minerals in bauxite: Gibbsite, bayerite and (pseudo-)boehmite, J. Colloid Interface Sci. 296 (2006) 572–576, https://doi.org/10.1016/j.jcis.2005.09.054.
[38] P. Cornette, S. Zanna, A. Seyeux, D. Costa, P. Marcus, The native oxide film on a model aluminium-copper alloy studied by XPS and ToF-SIMS, Corros. Sci. 174 (2020) 108837, https://doi.org/10.1016/j.corsci.2020.108837.
[39] A.E. Hughes, R.J. Taylor, B.R.W. Hinton, Chromate conversion coatings on 2024 Al alloy, Surface Interface Anal. 25 (1997) 223–234. 10.1002/(SICI)1096-9918(199704)25:4<223::AID-SIA225>3.0.CO;2-D.
[40] Y. bo Hu, X. yan Li, Influence of a thin aluminum hydroxide coating layer on the suspension stability and reductive reactivity of nanoscale zero-valent iron, Appl. Catal. B 226 (2018) 554–564, https://doi.org/10.1016/j.apcatb.2017.12.077.
[41] T. Gross, D. Treu, E. Ünveren, E. Kemnitz, W.E.S. Unger, Characterization of Cr „ III … Compounds of O , OH , F and Cl by XPS, 123 (2011) 77–123. 10.1116/11.20080801.
[42] M.C. Biesinger, B.P. Payne, A.P. Grosvenor, L.W.M. Lau, A.R. Gerson, R.S.C. Smart, Resolving surface chemical states in XPS analysis of first row transition metals, oxides and hydroxides: Cr, Mn, Fe, Co and Ni, Appl. Surf. Sci. 257 (2011) 2717–2730, https://doi.org/10.1016/j.apsusc.2010.10.051.
[43] S. Barnie, J. Zhang, P.A. Obeng, A.E. Duncan, C.D. Adenutsi, L. Xu, H. Chen, Mechanism and multi-step kinetic modelling of Cr(VI) adsorption, reduction and complexation by humic acid, humin and kerogen from different sources, Environ. Sci. Pollut. Res. 28 (2021) 38985–39000, https://doi.org/10.1007/s11356-021-13519-z.
[44] J. Zhang, H. Yin, H. Wang, L. Xu, B. Samuel, F. Liu, H. Chen, Reduction mechanism of hexavalent chromium by functional groups of undissolved humic acid and humin fractions of typical black soil from Northeast China, Environ. Sci. Pollut. Res. 25 (2018) 16913–16921, https://doi.org/10.1007/s11356-018-1878-5.
[45] P.C. Bandara, J. Peña-Bahamonde, D.F. Rodrigues, Redox mechanisms of conversion of Cr(VI) to Cr(III) by graphene oxide-polymer composite, Sci. Rep. 10 (2020) 1–9, https://doi.org/10.1038/s41598-020-65534-8.
[46] L.Q. Guo, S.X. Qin, B.J. Yang, D. Liang, L.J. Qiao, Effect of hydrogen on semiconductive properties of passive film on ferrite and austenite phases in a duplex stainless steel, Sci. Rep. 7 (2017) 8–13, https://doi.org/10.1038/s41598-017-03480-8.
[47] B.M. Weckhuysen, I.E. Wachs, R.A. Schoonheydt, Surface Chemistry and Spectroscopy of Chromium in Inorganic Oxides, 1996.
[48] A. De Luca, F. Senatore, A. Greco, Issues related to SPR joints subjected to fatigue loads, in: AIP Conf Proc, 2016. 10.1063/1.4949737.

[49] D.A. Davidson, Surface condition impacts part performance. Burrs, edges can negatively influence function of components, Metal Finishing 105 (2007), https://doi.org/10.1016/S0026-0576(07)80078-X.
[50] J.M. Hu, J.Q. Zhang, C.N. Cao, Determination of water uptake and diffusion of Cl- ion in epoxy primer on aluminum alloys in NaCl solution by electrochemical impedance spectroscopy, Prog. Org. Coat. 46 (2003) 273–279, https://doi.org/10.1016/S0300-9440(03)00010-9.
[51] J.-M. Hu, J.-T. Zhang, J.-Q. Zhang, C.-N. Cao, A novel method for determination of diffusion coefficient of corrosive species in organic coatings by EIS, J. Mater. Sci. 39 (2004) 4475–4479, https://doi.org/10.1023/b:jmsc.0000034140.96862.1a.
[52] Z. Manoli, D. Pecko, G. Van Assche, J. Stiens, A. Pourkazemi, H. Terryn, Transport of electrolyte in organic coatings on metal, in: Paint and Coatings Industry, IntechOpen, 2019. 10.5772/intechopen.81422.
[53] G.K. Van Der Wel, O.C.G. Adan, Moisture in organic coatings - a review, Prog. Org. Coat. 37 (1999) 1–14, https://doi.org/10.1016/S0300-9440(99)00058-2.
[54] S. Morsch, S. Emad, S.B. Lyon, S.R. Gibbon, M. Irwin, The location of adsorbed water in pigmented epoxy-amine coatings, Prog. Org. Coat. 173 (2022) 107223, https://doi.org/10.1016/j.porgcoat.2022.107223.
[55] F.H. Scholes, S.A. Furman, A.E. Hughes, T. Nikpour, N. Wright, P.R. Curtis, C.M. Macrae, S. Intem, A.J. Hill, Chromate leaching from inhibited primers. Part I. Characterisation of leaching, Prog. Org. Coat. 56 (2006) 23–32, https://doi.org/10.1016/j.porgcoat.2006.01.015.
[56] S.A. Furman, F.H. Scholes, A.E. Hughes, D. Lau, Chromate leaching from inhibited primers. Part II: Modelling of Leaching, Prog. Org. Coat. 56 (2006) 33–38, https://doi.org/10.1016/j.porgcoat.2006.01.016.
[57] T. Prosek, D. Thierry, A model for the release of chromate from organic coatings, 49 (2004) 209–217. 10.1016/j.porgcoat.2003.09.012.
[58] L. Xia, E. Akiyama, G. Frankel, R. McCreery, Storage and release of soluble hexavalent chromium from chromate conversion coatings equilibrium aspects of Cr [sup VI] concentration, J. Electrochem. Soc. 147 (2000), https://doi.org/10.1149/1.1393568.
[59] L. Xia, R.L. McCreery, Chemistry of a chromate conversion coating on aluminum alloy AA2024-T3 probed by vibrational spectroscopy, J. Electrochem. Soc. 145 (1998), https://doi.org/10.1149/1.1838768.
[60] J. Zhao, L. Xia, A. Sehgal, D. Lu, R.L. McCreery, G.S. Frankel, Effects of chromate and chromate conversion coatings on corrosion of aluminum alloy 2024–T3, Surf. Coat. Technol. 140 (2001) 51–57, https://doi.org/10.1016/S0257-8972(01)01003-9.
[61] J.D. Ramsey, R.L. McCreery, In situ Raman microscopy of chromate effects on corrosion pits in aluminum alloy, J. Electrochem. Soc. 146 (1999) 4076–4081, https://doi.org/10.1149/1.1392594.